FACULTAD DE CIENCIAS DEL MAR

UNIVERSIDAD DE LAS PALMAS DE GRAN CANARIA

LAGRANGIAN EVOLUTION OF A MID OCEAN ANTICYCLONIC EDDY

ELISABET RODRÍGUEZ CRUZ

Curso 2014/2015

PABLO SANGRÀ INCIARTE

DIANA GRISOLÍA SANTOS

Trabajo Fin de Título para la obtención del título en el Grado de Ciencias del Mar

LAGRANGIAN EVOLUTION OF A MID OCEAN ANTICYCLONIC EDDY

- Datos del Estudiante:
  Nombre: Elisabet Rodríguez Cruz
  Titulación que cursa: Grado en Ciencias del Mar
  Curso: 4º Curso
  Créditos superados: 210 ECTS
  Institución universitaria: Universidad de Las Palmas de Gran Canaria

- Datos del Tutor:
  Nombre: Pablo Sangrà Inciarte
  Departamento: Física
  Empresa: Instituto de Oceanografía y Cambio Global (IOCAG)

- Datos del Co-Tutor:
  Nombre: Diana Grisolía Santos
  Departamento: Física
  Empresa: Instituto Universitario de Oceanografía y Cambio Global (IOCAG)

- **Proyecto**: PUMP (CTM2012-33355).
- **Financiado por**:. Ministerio de Economía y Competitividad

Firma estudiante: Firma Tutor: Firma Co-Tutor:

Índice

Lagrangian evolution of a mid ocean anticyclonic eddy

[1]Elisabet Rodríguez-Cruz, [1]Pablo Sangrà, [1]Diana Grisolía

[1] Instituto de Oceanografía y Cambio Global (IOCAG).

Universidad de Las Palmas de Gran Canaria

Abstract

The lagrangian evolution of 4 months old anticyclonic intrathermocline eddy of the Canary Eddy Corridor is investigated from the trajectories of 5 satellites tracked drifting buoys. Buoys were drogued below and above the Ekman depth at 15 m and 100 m, respectively. One buoy remained inside the eddy during almost 4 months being thus a long lived coherent feature with a life span of at least 8 months. The eddy consisted in a central core rotating in solid body rotation with a rather constant periodicity of 4 days and in an outer ring rotating much more slowly with periodicities between 8 and 12 days. It translated westward with a slight equatorward deflection at an average speed of 3.5 km day^{-1} which is close to the phase speed of nondispersive baroclinic Rossby waves for this latitude, being thus strongly nonlinear. Buoys orbital radius variability analysis indicates that the eddy is elliptical and that its experience successive stages of increasing ellipticity followed by axisymetrization which is indicative of submesoscale filamentation. This analysis also reveals that when a surface drogued buoy converges toward the eddy center, a deep drogued buoy diverges toward the eddy periphery and vice versa. We propose that this is related with the switching of the secondary circulation between upwelling a downwelling modes being its periodicity of c.a. 20 days. This was observed for the first 65 days, in the rest of the period, the buoys orbital radius also fluctuates but in phase, indicating that the eddy also evolves pulsating increasing and decreasing its radius.

1. Introduction

Mesoscale eddies are nearly ubiquitous features of the World Ocean (Chelton et al., 2007, 2011). They occupy the 25 % of the ocean surface at any time (Chaigneau et al., 2009). They may be viewed as frontal structures with nearly circular shape. Therefore they isolate physical and biogeochemical properties at their interior and introduce gradients of those properties at their periphery, while they are advected. Their radius varies with the first baroclinic Rossby radius of deformation which is O (100-50 km) for low and mid latitudes and O (10 km) for high latitudes (Chelton et al., 1998). There are mainly three eddy types: cyclones, anticyclones and intrathermocline eddies (e.g. McGillicuddy et al., 2007). Due to the geostrophic adjustment, cyclonic eddies are recognizable by the upward doming of the isopycnals, while anticyclones are recognizable by their downward displacement. Intrathermocline eddies, also often referred as mode-water eddies, are a particular type of anticyclonic eddies being their most remarkable feature the associated dome shape of the isopycnals in the shallower layers and bowl shape in the deeper layers forming thus lens-like structures overall.

A 10 percent of the global eddy population are long-lived structures with lifetimes $\geq$ 4 months (Chelton et al., 2007, 2011; Sangrà et al., 2009). They have an average lifetime of 32 weeks and an average propagation distance of 550 km (Chelton et al., 2011). They propagate nearly due westward at approximately the phase speed of nondispersive baroclinic Rossby waves with preferences for slight poleward and equatorward deflection of cyclonic and anticyclonic eddies, respectively (Chelton et al., 2011). Long lived anticyclones slightly dominate over cyclones. The Canary Archipelago is a continuously source of mesoscale eddies as consequence of prevailing currents and winds perturbation by the islands topography (Arístegui et al., 1994; Sangrà et al., 2005, 2007, 2009). Sangrà et al. (2009) observed that Canary Island induced eddies contribute to a zonally oriented long lived eddy corridor that can extend as far as the Mid Atlantic Ridge; this was named as the Canary Eddy Corridor. It constitutes a major pathway for long lived eddies in the northeastern subtropical Atlantic. Long lived anticyclonic eddies clearly dominate over cyclonic eddies. As observed by Chelton et al (2011) for global eddies those anticyclones propagates westward with a slight equatorward deflection.

It is well known that mesoscale eddies modulate biological production and related biogeochemical fluxes (Benitez-Nelson et al., 2007; McGillicuddy et al., 2007; Lévy, 2008). In particular, long lived anticyclonic eddies may exert a profound influence on phytoplankton. In this regard there are growing evidences that point out that anticyclonic eddies may be more productive than cyclones (McGillicuddy et al., 2007; Gaube et al., 2013, 2014). Therefore the classical view that anticyclones are oligotrophic structures while cyclones are productive structures is being abandoned. Self-induced Ekman pumping, as a consequence of eddy-wind interaction, may lead to upwelling in the interiors of anticyclonic eddies (Martin and Richards, 2001; McGillicuddy et al., 2007; Gaube et al., 2013). This will lead to an increase of primary production through nutrient injection to the euphotic zone at eddies centers. Eddy-wind interaction through nonlinear Ekman pumping may also enhance primary production at eddy peripheries (Mahadevan et al., 2008). Other mechanisms that can enhance primary production in anticyclones are the upwelling generated during the decay of anticyclones, often referred to as ‘‘eddy pumping’’ (Falkowski et al., 1991), the stirring of the ambient chlorophyll field by advecting phytoplankton around eddy peripheries (Siegel et al., 2007, 2011; Chelton et al., 2011b), and the eddy trapping of high productive waters during their generation (Lehahn et al., 2011; Early et al., 2011). Sangrà et al. 2005 suggested that anticyclones inside of the Canary Eddy Corridor may account for a total primary production as high as the Northwest African Upwelling system at the same latitude range.

There are very few studies on the lagrangian evolution of the Canary Eddy Corridor anticyclones. In an earlier study Pingree (1996) surveyed an anticyclonic eddy located in the middle of the Canary Eddy Corridor near 27ºN, 22º W and deployed three Argos buoys drogued at ca. 200 m. One buoy tracked the eddy during ca. 16 months along a 1650 km westward trip. The initial rotating period was of 8 days then increasing to 5 days due to its subducting character. This author described the eddy as a shallow subtropical subducting westward propagating eddy and named it as Swesty. Sweesties are mode water of intrathermocline eddy type. Sangrà et al. (2005) described during 7 months the life story of an anticyclonic eddy shed by Gran Canaria Island from the trajectories of 3 Argos buoys drogued at 100 m depth. It drifted southwestward up to 500 km with the mean Canary Current. The eddy evolved from a young stage, where the core retains its vorticity and occupies most of the eddy being in solid body rotation, through a mature stage, where the eddy has a reduced inner core and a slowly revolving outer ring, to a decay stage, where the vorticity maximum is substantially reduced. Rotating rates varies from 3 days for the young stage to 6 days for the mature and decay stages. The eddy evolved pulsating decreasing and increasing its radius.

A typical anticyclonic eddy of the Canary Eddy Corridor named as the eddy PUMP, located 300 nautical miles southwest of the Canary Islands, was interdisciplinary surveyed on September 2014 in the framework of the PUMP project (ref: CTM2012-33355). This project aims to investigate the modulation of the biogeochemical fluxes by the ageostrophic secondary circulation (SAC) and mixing in anticyclonic mesoscale eddies. The eddy, 4 months old, was an intrathermocline type eddy characterized by a dome shape of the isopycnals in the sallower layers and bowl shape in the deeper layers. It was elliptical, 110 km diameter and 400 m deep. This study aims to describe lagrangian evolution of this eddy from 6 drifting buoys trajectories. As it will be showed it will provide news insight on this evolution such as the occurrence of axisymetrization episodes or the switching between upwelling and downwelling modes.

2. Methodology

2.1. PUMP eddy survey and buoys deployment

In the framework of the PUMP project an anticyclonic eddy was surveyed from 04 to 20 of September 2014. Figure 1 depicts the eddy location in September 13, as obtained from merged altimetry AVISO data. It was generated by Tenerife Island four months before the survey, hence being four months old. Its signal is easily recognizable by a strong positive sea level anomaly (SLA) 300 nautical miles (nm) southwest of the Canary Island inside the Canary Eddy Corridor (CEC; Sangrà et al., 2009). As already introduced, the CEC is built up by the Canary Islands induced eddies as consequence of prevailing wind (Trades winds) and currents (Canary Current) perturbation. Long lived (life span > 4 months) anticyclonic eddies are more frequent than long lived cyclones due to their higher initial rotating rate (Sangrà et al., 2007). The PUMP eddy can be viewed as a typical anticyclonic eddy of the CEC.

As part of the cruise strategy we conducted a high resolution meridional transect named as "Le Tourmalet", crossing the eddy center (Figure 2). As indicated in Table 1 and illustrated in Figure 2 we deployed 6 buoys along this transect at different distances from the eddy center. Three buoys (buoys 01, 02 and 06) were drogued inside the Ekman layer (15 m) and three (buoys 03, 04 and 05) below the Ekman layer (100 m). Drogues were a holey sock type with 1 m of diameter and 15 m of longitude. Position data were transmitted through the SPOT satellite messenger system which is a low cost system with a yearly flat rate. Averaged time resolution was about 1 hour.

2.2. Estimating the eddy center trajectory

Eddy center trajectory is calculated using a method proposed by Brassington, G. B. (2009) based on that, the lagrangian trajectory given by a buoy inside the eddy exhibits an oscillatory motion. In that way, plotting each orthogonal coordinate of the time series position will provide two extremun points per completed orbit that will correspond to the northern and southern points for the meridional coordinate and the eastern and western points for the zonal one (Figure 6). The maxima and minima for each coordinate will be interpolated in order to get the extrema for each instant of time. Its averaging will give us the eddy center trajectory.

To apply this method to our data, we selected buoys 5 and 6 as their remained the longest time inside the eddy and in addition one was drogued at 100 m (buoy 5) and other at 15 m (buoy 6). Only data while the buoys remained inside the eddy were considered. Buoys position will be treated separately for each coordinate. Firstly, we worked with RAW data, taking the deployment date, 14 of September, as the day zero (*t=0*) at 02:00 local hour of Madrid and we removed outlayers. Data had to be filtered using a low pass butterworth filter to remove inertial oscillations with a cut-off frequency of two days.

The next step consists in interpolating the extrema for each coordinate. Once the extrema are identified from the filtered time series, as shown (Figure 4), it is applied a cubic spline interpolation to maxima and minima points separately. Figure 5 shows the interpolated curves obtained for each coordinate. As it can be seen from this Figure, the beginning and the end of the interpolated curves for the extrema do not fit in time, given that the maxima and minima of the series start at different times. Therefore, due to both a maximum and a minimum is necessary to compute the eddy center position at a given time, the interpolated data which start in the first minima to last maxima will be used corresponding to 16 of September of 2014 at 20:00 to 13 of February of 2015 at 07:00 for buoy 5 and to 18 of September of 2014 at 08:00 to 29 of January of 2015 at 20:00 for buoy 6. Figure 7 shows the eddy center trajectory and the buoy position for buoy 6 and buoy 5.

3. Results

3.1. Buoys trajectories and mean periods

Figure 3 illustrated buoy´s trajectories while they remain inside the eddy. Buoy 1 only transmitted its position during 6 days hence it was discarded for the analysis. Buoy 2 drogued at 15 m depth remained inside the eddy during ca. 32 days tracing 4 loops (Table II). Its trajectory indicates that during these first 25 days the eddy translates westward. Eddies self-translates westward due to the gradient of planetary vorticity (β-effect) along its radius (Cushman-Roisin, 1994; Van Leeuwen, 2007). This induces a net Coriolis force that must be compensated by a gradient pressure force that forces the eddy westward displacement. Eddies trajectory will also rely on their interaction with the mean flow (Cushman-Roisin, 1994). In this regard, the westward propagation of the eddy suggests that during this first period self-westward translation dominates over the background flow advection indicating that this later must be relatively low.

From a detailed inspection of the buoy 2 trajectory, we can notice smalls near closed loops superposed to the mains loops. These are the signature of near inertial waves (NIW). Trapping of NIW by anticyclonic eddies has been predicted theoretically and observed for anticyclonic eddies close to the Canary Islands (Kunze, 1985; Lueck and Thomas, 1986; Martínez-Marrero et al., 2014). Inside the eddy, the frequency of the NIW is reduced by the negative value of the eddy relative vorticity. Then the resulting frequency value for NIW inside the eddy will be below the inertial value, determined by the latitude. This will cause that NIW reflect as they reach the eddy boundary resulting on its trapping by the eddy.

Buoy 6, also drogued at 15 m, was the one that remained more time inside the eddy tracking, 13 loops during 145 days (Figure 3, Table II). Its trajectory indicates that after the first 25 days the eddy translates southwestward until day 110 and then, it moves again westward. This suggests the occurrence of an intensification of the southward flowing Canary Current during days 25-110. Superposed small near closed loops associated to NIW are also noticeable all along this buoy trajectory. Buoy 3 and 4 drogued at 100 m remained 32 and 46 days inside the eddy, tracking 6 and 13 loops respectively (Table II). Buoy 5, also drogued at 100 m, together with buoy 6 remained more than three months inside the eddy drawing 36 loops along 123 days.

When the buoys where deployed the eddy was 4 months old. As buoy 6 remained inside the eddy during near four more months the eddy life span is at least 8 months being thus a long lived coherent structure. This indicates that this structure is stable to inertial perturbations. The inertial stability criteria depends on the eddy type, Rankine or Gaussian, and on its initial rotating period (Sangrà et al., 2007). We may obtain an approach to the eddy mean period dividing the number of buoys loops by the time-span while they remained inside the eddy (Table II). This period varies from 3.5 days for buoy 5 closer to the eddy center, to 11 days for buoys 6 orbiting at the eddy periphery. This indicates that the eddy was not in solid body rotation with an inner core rotating faster than the periphery, being thus a Gaussian type eddy. As we will discuss in section 4, these rotating rates for a Gaussian vortex render the eddy stable to inertial perturbation being thus able to evolve as a long lived coherent structure.

3.2. Eddy translation and orbits

The next parameters that we are going to describe have been only calculated for buoys 5 and 6, being those that remained more time inside the eddy as already mentioned. Figure 7a and b show the whole trajectory and the center eddy trajectories for these two buoys. Remember that centroids locations give us an approach to the eddy center displacement/trajectory or eddy translation. In both cases centroids positions cross the loops centers indicating that the methodology was well approached to the eddy center trajectory (Figure 7). Although this trajectory is similar for both buoys, there is some mismatch. There are some loops like displacements on buoy´s 5 eddy center trajectory that are not presented in buoy 6. This is probably related to high rotating rate of buoy 5, while the filter to remove high frequency variability was the same as for buoy 6. As already detailed from the whole trajectories analysis, eddy center trajectory indicate that initially it translates westward, then it moves southwestward probably due to its interaction with the Canary Current, and finally self-translates again westward.

Although mean eddy center speed for both buoys are similar, there is clearly mismatch for the instantaneous speed as shown is Figure 8. Time series for buoy 5 show a high frequency variability about 10 days of period which is not present in buoy 6 time series. This high frequency variability is related with the loops observed in the trajectory of the eddy center for buoy 5 mentioned above, being thus probably a methodological artifact. When this variability is filter out, both times series resembles with a rather constant velocity although with small amplitude low frequency variability.

We may obtain the buoys orbits around the eddy center subtracting the eddy center trajectory (eddy drift) to the whole trajectory (Figure 9). This will allow us to describe the lagrangian properties of the eddy removing the translation effects. Orbits for the interior buoy (buoy 5) show a near circular shape with maximum radius of ca. 10 km indicating that this buoy remained very close to the eddy center for the 123 days period (Figure 9a). It described 36 clockwise near circular revolutions around the eddy center being thus its mean period about 3.4 days (Table II). Buoy 6, located at the eddy periphery, describes only 13 revolutions along a 145 days period being thus the mean period much lower, ca. 11 days (Figure 9b). This confirm that the eddy is a Gaussian type, where the periphery rotates much slower than the eddy core. Outer orbits of buoy 6 are elliptical with the major axis oriented zonally, being their maximum radius about 50 km.

3.3. Orbital Radius

Figure 10 displays the instantaneous and mean (9 days) orbital radius for the two buoys. This mean radius has been obtained with a low-pass filter of the instantaneous values (1 hour data) using a Lanczos filter with a 9 days cutoff period. In all cases the instantaneous radius fluctuates around a slowly changing mean value, which indicates that the buoy orbits are elliptical. Notice that those elliptical related fluctuations are of higher frequency and smaller amplitude for the inner buoy (buoy 5). Notice also, that there is an increase of the amplitude of the fluctuations between days 50 and 100 and then a decrease again. This is suggestive that the eddy in a first stage loses its nearly circular shape, gaining ellipticity and then suffering a process of axisymmetritation recovering finally its initial near circular shape.

Times series for the mean orbital radius indicates that instead to be constant their show a clearly low frequency variability (Figure 10). A striking feature is that during the first 65 days' time period evolution, the surface drogued buoy (buoy 5, 15 m) and the subsurface drogued buoy (buoy 6, 100 m) mean orbital radius were in opposite phase. When the buoy 5 orbital radius decreases, the orbital radius for buoy 6 increases and vice versa. After day 65 both mean orbital radius show the same tendency. First there is a tendency for increasing radius and then a tendency for it decreases. This is suggestive that the eddy evolves also pulsating. Eddies pulsations along its time evolution has been already described for the Canary Eddy Corridor eddies being a common feature (Sangrà et al., 2005, 2009).

3.4 Velocities and periods

A view of the temporal evolution of the eddy rotation rate may be obtained from either Cartesian components of the buoys' horizontal velocities (Sangrà et al., 2005). Uppers panels of Figure 11 shows the zonal component of velocity (eastward positive) for all two buoys as obtained from the 60 hours smoothed time series being thus NIW signals filtered out. The evolution of the zonal velocity contains both information about the rotating period of the eddy and its position relative to the center. Lowers panels of Figure 11 show the corresponding wavelet analysis (e.g. Percival and Walden, 2000) for zonal velocities. As indicated in Sangrà et al (2005), the wavelet power spectrum is defined as the squared absolute value of the wavelet transform and gives a measure of the temporal evolution of the time series variance for all periods. The contours correspond to kinetic energy density, in exactly the same manner as the energy spectra, and provide information of the energy level at each frequency. The sharpness of the peak energy is indicative of the rotation stability rate, while a peak that remains sharp but decreases in intensity reflects a smaller rotation radius.

Wavelet analysis for buoy 5 shows that initially the period increases from 3 to 4 days and then it remains quite constant for the rest of the period (Figure 11a). The peak energy is quite sharp denoting a rather stable rotation rate. However peaks intensity is far from be constant, reflecting a variable rotation radius as discussed above and depicted in Figure 10. Between days 20 and 40 and between days 50 to 70, kinetic energy density is very low, coinciding with very small amplitudes of the zonal velocity. Orbital radius time series for this buoy shows that is consistent with a radius decrease being the buoys very close to the eddy center. It is important to notice that from day 20 the rotation rate remains almost constant, 4 days, in spite that the radius varies between 5 and 15 km (Figure 10). This indicates that the central core of the eddy was in solid body rotation

As expected the rotation rate for the buoy 6, located at the eddy periphery, is lower for those corresponding to the interior buoy ranging from 8 to 12 days (Figure 11 b). Therefore the inner core of the eddy rotates threefold faster than its outer ring. Zonal velocity time series for this periphery buoy shows that its oscillating nature is rather more instable than those, corresponding with the interior buoy. This is also evident in the wavelet analysis where the energy peaks are broader than in the case of the interior buoy. The wavelet analysis shows that during the firsts 90 days the period increase monotonically from 8 to 12 days, being stable for the first 40 days and then becoming instable. Between days 90 and 110 there is a jump which is suggestive that the buoy has leaved the eddy. It enters again in the eddy by day 110 experiencing a rotating rate of 9 days before leaving it definitively the eddy. A striking feature is between day 35 and 50 that the orbital radius decrease but the rotation rate continues to increase. This may be related with a deceleration of the eddy or with a methodological artifact.

4. Discussion

Eddy PUMP was generated by the Tenerife Island 4 months before the buoys deployment. Once deployed, one of the buoys tracked the eddy during 4 more months. Therefore the life span of the PUMP eddy is at least 8 months being thus a long lived coherent structure. As proposed by Sangrà et al. (2007) the high life expectancy of anticyclonic eddies in the Canary Eddy Corridor is related to their Rankine like nature at the time of its generation. Rankine vortices rotate in solid body rotation. In this case a cyclonic/anticyclonic circulation develops at the periphery of anticyclones/cyclones that renders anticyclones/cyclones stables/unstable to inertial perturbations. Sangrà et al. (2007) predicted that maximum initial rotating rate for anticyclones to be stable is 2.5 days whereas is much lower for cyclones being 4.5 days. In this regard Piedeleu (2014) observe a rotating rate of 3 days for anticyclones close to the origin island and 5 days for cyclones, confirming also their Rankine like type. It is expected that the eddies cores retains its initial rotating rate. In the case of the eddy PUMP the rotation rate for the core is between 3 and 4 days, very close to those predicted for the anticyclones at the time of its generation. Therefore we propose that the long lived character of the eddy PUMP is related with its initial Rankine like type and with an initial maximum rotation rate permitted by the inertial instability about 3 days. The dominance of long lived anticyclones is a general feature of eddies inside the Canary Eddy Corridor (Sangrà et al., 2007).

Sangrà et al. (2005) studied the lagrangian evolution of an anticyclonic eddy during seventh months since its origin at the Canary Island. Al already introduced, they observed three stage of evolution: a young stage where the eddy was in solid body rotation being a Rankine-like eddy, a mature stage where the eddy evolves to a Gaussian type with an inner core, retaining its initial rotation while the outer ring rotating much more slowly, and finally a decay stage where it exists a diffusion of vorticity. Inferences and direct estimates from wavelet analysis indicate that the PUMP eddy core was rotating threefold faster than the periphery and also indicate that the core was in nearly solid body rotation. Therefore, as for the eddy described by Sangrà et al. (2005) in its mature stage, PUMP eddy consist on an inner core that probably retains its initial rotating rate and an outer ring that rotate much more slowly being thus a Gaussian type eddy. To be stable Gaussian vortices absolute value of the angular velocity may not exceed the planetary vorticity, $|\omega|<f/2$ (Sangrà et al. 2007). This criteria is matched for the PUMP eddy when taking the higher rotating rate (3.5 days), $|\omega|$ ($2\cdot10^{-5}$ s^{-1}) $<f/2(3\cdot10^{-5}s^{-1})$. Therefore the PUMP eddy is also stable in this mature stage explaining also it large life span.

Chelton et al. (2007) from a global eddies census observed that eddies propagate nearly due westward at approximately the phase speed of nondispersive baroclinic Rossby waves, with preferences for slight poleward and equatorward deflection of cyclonic and anticyclonic eddies, respectively. This is the case for our PUMP eddy. An approach to the eddy mean translation speed may be derived from the eddy center trajectory as depicted in Figure 7. Mean speed for the eddy center displacement for both buoys is 3.5 km day^{-1} which is close to the phase speed of nondispersive baroclinic Rossby waves for this latitude (Chelton et al., 2007). In this regard, eddies whose translation speed is much less than the average mean speed within the interior of eddies, *U*, are named as nonlinear eddies (Chelton et al., 2007; Chelton et al., 2011). An important property of nonlinear eddies is that they can trap waters at their interior (McWilliams and Flierl, 1979; Flierl, 1981). Another related important property is that the ecosystem carried by a nonlinear eddy is isolated from the background waters (Gaube et al., 2014). Eddy PUMP is strongly nonlinear as the mean speed within the interior of the eddy or mean rotational speed, 0.1 ms^{-1}, that greatly exceed the mean translation speed 0.04 ms^{-1} (3.5 km day^{-1}).

As we have described in section 3.3, orbital radius high frequency variability suggest that eddy evolves through successive stages of ellipticity an axisymetrization. Numerical studies point out that a mesoscale eddy gain ellipticity when it becomes instable (e.g. Melander et al., 1987; Koumoutsakos, 1997). As consequence, two submesoscale filaments develops at the ellipse vertex. These filaments will grow as the instability progress causing the axisymmetritation and filamentation of the vortex, returning to its near circular shape. Therefore the evolving stage between elliptical and axisymmetritation modes of the PUMP eddy are suggestive of the development of submesoscale filaments. This may have important consequences for modulating biogeochemical fluxes as intense vertical velocities may develop in those submesoscale frontal structures (e.g. Klein and Lapeyre, 2009).

As already mentioned and shown in Figure 10, and striking feature of the mean orbital radius evolution is the opposite phase evolution of the surface and subsurface buoys. This indicates that a surface convergence/divergence (buoy 6) coincides with a subsurface (buoy 5) divergence/convergence. As depicted in Figure 12, a divergence in the surface layers and a convergence in the lower layers may be suggestive of upwelling whereas the opposite may be suggestive of downwelling. Therefore during this first 65 days period, the mean orbital radius variability is suggestive that the eddy PUMP is switching between upwelling and downwelling modes with a ca. 20 days periodicity.

5. Summary and conclusions.

We deployed 5 drifting boys in 4 months old anticyclonic eddy, named as the eddy PUMP, inside the Canary Eddy Corridor in order to investigate its lagrangian evolution. Buoys were drogued above (15 m) and below (100m) the Ekman layer depth. One buoy remained inside the eddy during 143 day indicating a life span for the eddy of at least 8 months, being thus a long lived structure. We propose that this long lived character is related with a high rotating rate during its birth, probably linked with its Rankine like behavior and with the fact that this rotating rate does not exceed the threshold for inertial instability when it evolves as a Gaussian vortex type.

A wavelet analysis of the zonal velocities for the buoy that remained close to the eddy center reveals that the core of the eddy was in solid body rotation with a rather constant period of 4 days all along the 123 days that the buoy remained inside the eddy. This is suggestive that the eddy evolves losing little kinetic energy and enstrophy which is in accordance to its long lived character. The buoy located near the periphery increases monotonically its rotating period from 8 to 12 days as its mean orbital radius increases indicating that that eddy rotation rate decrease gradually as we approach the eddy outer ring. This is typical behavior of a Gaussian type eddy. Therefore eddy PUMP consist on an inner core that probably retains its initial rotating rate and outer ring that rotate much more slowly being thus a Gaussian type. Superposed to the instantaneous trajectories we observed the signal of near inertial waves being suggestive that the eddy act trapping those waves as predicted by theoretical studies and observations (Kunze, 1985; Lueck and Thomas, 1986; Martínez-Marrero et al., 2014)

The PUMP eddy mean translation was westward with a mean speed ca. 3.5 km day^{-1}. As observed for global eddies this speed is close to the phase speed of nondispersive baroclinic Rossby waves. This speed is much less than the mean rotational speed of the eddy (0.2 ms^{-1}) being thus a nonlinear eddy. This is an important characteristic as water is trapped in the interior of nonlinear eddies having thus important consequences for the biogeochemical fluxes. Related with this we observed from the mean orbital radius variability that the eddy is elliptical and that its experience successive stages of increasing ellipticity followed by axisymetrization. This may be a sign of the development of submesoscale filament where the secondary circulation may be intense and thus playing an important role on modulating biogeochemical fluxes.

Mean buoys orbital radius evolution reveals that when a surface drogued buoy converge toward the eddy center, a deep drogued buoy diverges toward the eddy periphery and vice versa. This is suggestive of two process first the occurrence of upwelling and downwelling and second the alternation of these process with a periodicity of ca. 20 days. Therefore the PUMP eddy switches between upwelling and downwelling modes along its time evolution. We have also observed that the eddy evolves pulsating reflected by the phase increasing and decreasing of the buoys mean orbital radius. This may also have important consequences for the ecosystem trapped inside the eddy and related biogeochemical fluxes.

Acknowledgements

We express our gratitude to the technical staff (UTM-CSIC) and crew of R/V BIO Hespérides for supporting our work at sea. This work was supported by the Spanish government through project PUMP (CTM2012-33355).

References

Arístegui, J., Sangrà, P., Hernández-León, S., Cantón, M., Hernández-Guerra, A., Kerling, J. L., (1994). Island-induced eddies in the Canary Islands. *Deep-Sea Research I*, 44, 1509-1525.

Benítez-Nelson, C. R., Bidigare, R. R., Dickey, T. D., Landry, M. R., Leonard, C. L., Brown, S. L., Nencioli, F., Rii, Y. M., Maiti, K., Becker, J. W., Bibby, T. S., Black, W., Cai, W. J., Carlson, C. A., Chen, F., Kuwahara, W. S., Mahaffey, C., McAndrew, P. M., Quay, P. D., Rappe, M. S., Selph, K. E., Simmons, M. P., Yang, E. J., (2007). Mesoscale eddies drive increased silica export in the Subtropical Pacific Ocean. *Science*, 316, 1017–1021.

Brassington, G. B., (2010). Estimating surface divergence of ocean eddies using observed trajectories from a surface drifting buoy. *Journal of Atmospheric an Oceanic Technology*, 27, 705-720.

Chaigneau, A., Eldin, G., Dewitte, D., (2009). Eddy activity in the four major upwelling systems from satellite altimetry (1992–2007). *Progress in Oceanography*, 83(1), 117–123.

Cushman-Roisin, B., (1994). Introduction to geophysical fluid dynamics. *Prentice Hall*, 313 pp.

Chelton, D. B., Deszoeke, R. A., Schlax, M. G., Naggar, K., Stwertz N., (1998). Geographical variability of the first baroclinic Rossby radius of deformation. *Journal of Physical Oceanography*, 28, 433–460.

Chelton, D.B., Schlax, M.G., Samelson, R.M., de Szoeke, R. A., (2007). Global observations of large oceanic eddies. *Geophysical Research Letters*, 34, L15606.

Chelton, D., Schlax, M., Samelson, R., (2011). Global observations of nonlinear mesoscale eddies. *Progress in Oceanography*, 91(2), 167–216.

Chelton, D., Gaube, O., Schlax, M., Early, J., Samelson, R., (2011b). The influence of nonlinear mesoscale eddies on near-surface oceanic chlorophyll. *Science*, 334(6054), 328–332.

De Boor, C., (2001). A Practical Guide to Splines. Vol. 27, Applied Mathematical Sciences, 346 pp.

Duchon, C. E., (1979). Lanczos Filtering in one and two dimensions. *Journal of applied Meteorology*, 18, 1016-1022.

Early, J., Samelson, R., Chelton D., (2011). The evolution and propagation of quasigeostrophic ocean eddies. *Journal of Physical Oceanography*, 41(8), 1535–1555.

Falkowski, P., Ziemann, D., Kolber, Z., Bienfang, P., (1991). Role of eddy pumping in enhancing primary production in the ocean. *Nature*, 352(6330), 55–58.

Flierl, G. R., (1981). Particle motions in large-amplitude wave fields. *Geophysical Astrophysical Fluid Dynamics*, 18(1–2), 39–74.

Gaube, P., Chelton, D., Strutton, P., Behrenfeld, M., (2013). Satellite observations of chlorophyll, phytoplankton biomass and Ekman pumping in nonlinear mesoscale eddies. *J. Geophys. Res. Oceans*, 118, 6349–6370.

Gaube, P., McGillicuddy Jr., D. J., Chelton, D., Behrenfeld, M., Strutton, P., (2014). Regional variations in the influence of mesoscale eddies on near-surface chlorophyll. *Journal of Geophysical Research*, 119, doi: 10.1002/2014JC010111.

Klein, P., Lapeyre, G., (2009). The oceanic vertical pump induced by mesoscale and submesocale turbulence. *Annual Review of Marine Sciences*, 1, 351-375.

Koumoutsakos, P., (1997). Inviscid Axisymmetrization of an Elliptical Vortex. *Journal of Computational Physics*. 138, 821-857.

Kunze, E. T. B., (1985). Near-inertial wave propagation in geostrophic shear. *Journal of Physical Oceanography*, Vol. 15, pp. 544-565.

Lévy, M., (2008). The modulation of biological production by mesoscale turbulence. *Lecture Notes in Physics*, 744, 219–261.

Lehahn, Y., d'Ovidio, F., Levy, M., Amitai, Y., Heifetz, E., (2011). Long range transport of a quasi-isolated chlorophyll patch by an Agulhas ring. *Geophysical Research. Letters*, 38, L16610.

Lueck, R. and Thomas, O., (1986). The Dissipation of Kinetic Energy in a Warm-Core Ring. *Journal of Geophysical Research*, 91 (C1), 803-818.

Mahadevan, A., Thomas, L. N., Tandon, A., (2008). Comment on "Eddy/Wind Interactions Stimulate Extraordinary Mid-Ocean Plankton Blooms". *Science*, 320, 448b.

Martin, A. P. and Richards, K. J., (2001). Mechanisms for vertical nutrient transport within a North Atlantic mesoscale eddy. *Deep Sea Research II*, Vol. 48, pp. 757–773.

Martínez-Marrero, A., Sangrà, P., Caldeira, R. M., Aguiar-González, B. and Rodríguez-Santana, A., (2014). Observations of the interaction between near-inertial waves and mesoscale eddies. *EGU General Assembly 2014, Vienna, Austria.*

McGillicuddy, Jr., D. J., Anderson, L. A., Bates, N. R., Bibby, T., Buesseler, K. O., Carlson, C. A., Davis, C. S., Ewart, C., Falkowski, P. G., Goldthwait, S. A., Hansell, D. A., Jenkins, W. J., Johnson, R., Kosnyrev, V. K., Ledwell, J. R., Li, Q .P., Siegel, D. A., Steinberg, D.K., (2007). Eddy/Wind interactions stimulate extraordinary Mid-Ocean plankton Bloom. *Science*, Vol. 316, pp.1021–1026.

McWilliams, J., Flierl, G., (1979). On the evolution of isolated, nonlinear vortices.

Journal of Physical Oceanography, 9(6), 1155–1182

Melander, M. V., Zabusky, N. J. & McWilliams, J. C., (1988). Symmetric vortex merger in two dimensions: causes and conditions. *Journal of Fluid Mechanics*, 195, 305–340.

Percival, D. B., Walden, A., T., (2000). *Wavelet Methods for Time Series Analysis*, Cambridge University Press, New York.

Piedeleu, M., (2014). Remolinos oceánicos de las Islas Canarias: generación, características y evolución. PhD thesis, Universidad de Las Palmas de Gran Canaria, Spain.

Sangrà, P., Pelegrí, J. L., Hernández-Guerra, A., Arregui, I., Martín, J. M., Marrero-Díaz, A., Martínez, A., Ratsimandresy, A. W., Rodríguez-Santana, A., (2005). Life History of an anticyclonic eddy. *Journal of Geophysical Research*, 11, C03021.

Sangrà, P., Auladell, M., Marrero-Díaz, A., Pelegrí, J.L., Fraile-Nuez, E., Rodríguez-Santana, A., Martín, J. M., Mason, E. and Hernández-Guerra, A., (2007). On the nature of oceanic eddies shed by the Island of Gran Canaria. *Deep-Sea Research I*, 54, 687-709.

Sangrà, P., Pascual, A., Rodríguez-Santana, A., Machín, F., Mason, E., McWilliams, J. C., Pelegrí, J. L., Dong, C., Rubio, A., Arístegui, J., Marrero-Díaz, A., Hernández-Guerra, A., Martínez-Marrero, A. and Auladell, M., (2009). The Canary Eddy Corridor: a major pathway for long-lived eddies in the subtropical North Atlantic. *Deep-Sea Research I*, 56, 2100-2114.

Siegel, D., Court, D., Menzies, D., Peterson, P., Maritoena, S., Nelson, N., (2007). Satellite and in situ observation of the bio-optical signatures of two mesoscale eddies in the Sargasso Sea. *Deep Sea Research, Part II*, 55, 1218–1230.

Siegel, D., Peterson, P., McGillicuddy Jr., D. J., Maritorena, S., Nelson, N., (2011). Bio-optical footprints created by mesoscale eddies in the Sargasso Sea. *Geophysical Research Letters*, 38, L13608

Van Leeuwen, P. J., (2007). The propagation mechanism of a vortex on the plane. *Journal of Physical Oceanography*, Vol. 37, pp. 2316-2330.

BUOY ID	DROUGUE DEPTH (meters)	DATE	TIME (GMT)	LATITUDE	LONGITUDE
PUMP 03	100	13/09/14	03:17	26º 23.019’N	20º 20.067’W
PUMP 01	15		03:37	26º 22.014’W	20º 19.980’W
PUMP 05	100	13/09/14	08:30	26º 13.025’N	20º 20.018’W
PUMP 02	15		03:37	26º 11.975’W	20º 19.976’W
PUMP 04	100	13/09/14	13:57	26º 07.980’N	20º 19.845’W
PUMP 06	15		14:13	26º 08.736’W	20º 19.950’W

Table I. Deployment characteristics of the drifting buoys.

Buoy	Loops	Time span (days)	Mean period (days)
02	*4*	*32.5*	*8.1*
06	*13*	*145*	*11.1*
03	*6*	*32.5*	*5.4*
04	*13*	*46*	*3.5*
05	*36*	*123*	*3.4*

Table II. Buoys trajectory inferred parameters.

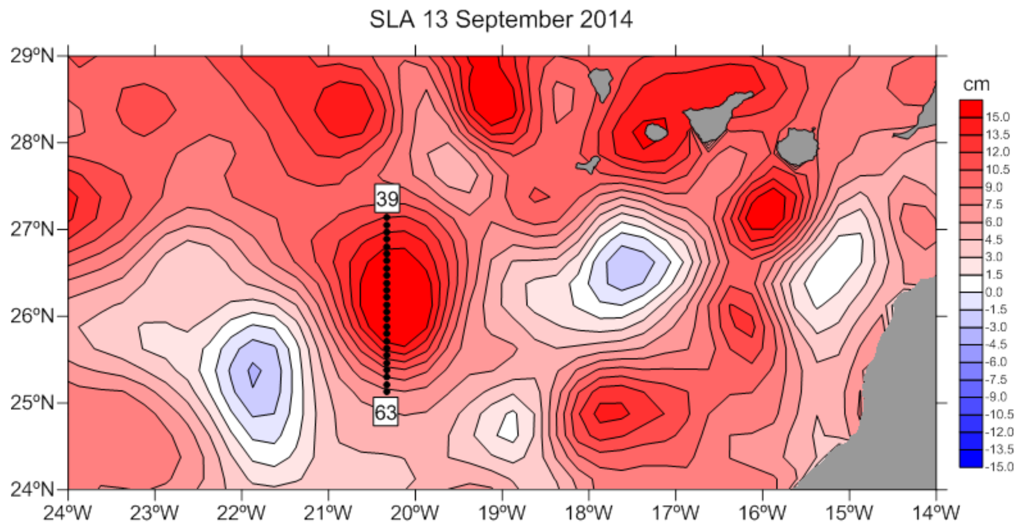

Figure 1. Sea Level Anomaly (SLA) image from aviso, showing the location of the anticyclonic eddy PUMP. Black dots indicate CTD stations along a transect crossing the eddy, which was named as "Le Tourmalet". Station numbers at the transect end are also indicated.

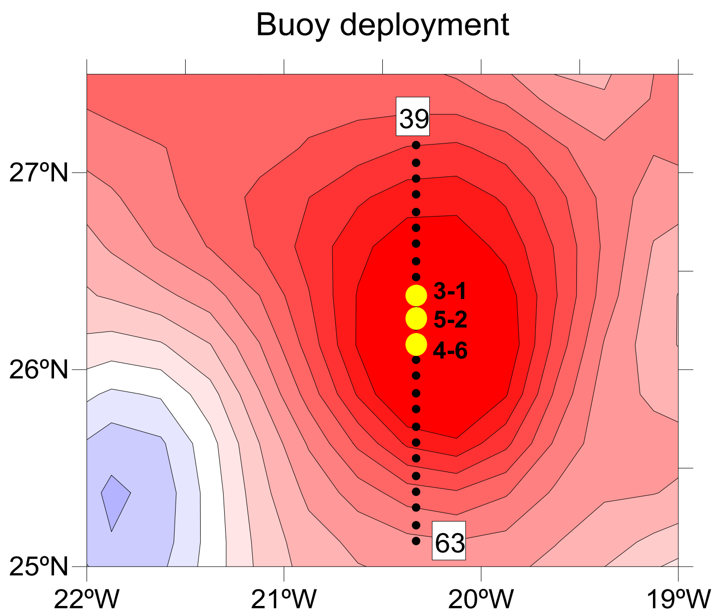

Figure 2. Buoys deployments location (yellow dots) superposed to 13 of September of 2014 SLA image. "Le Tourmalet" transect CTD stations are indicating by black dots.

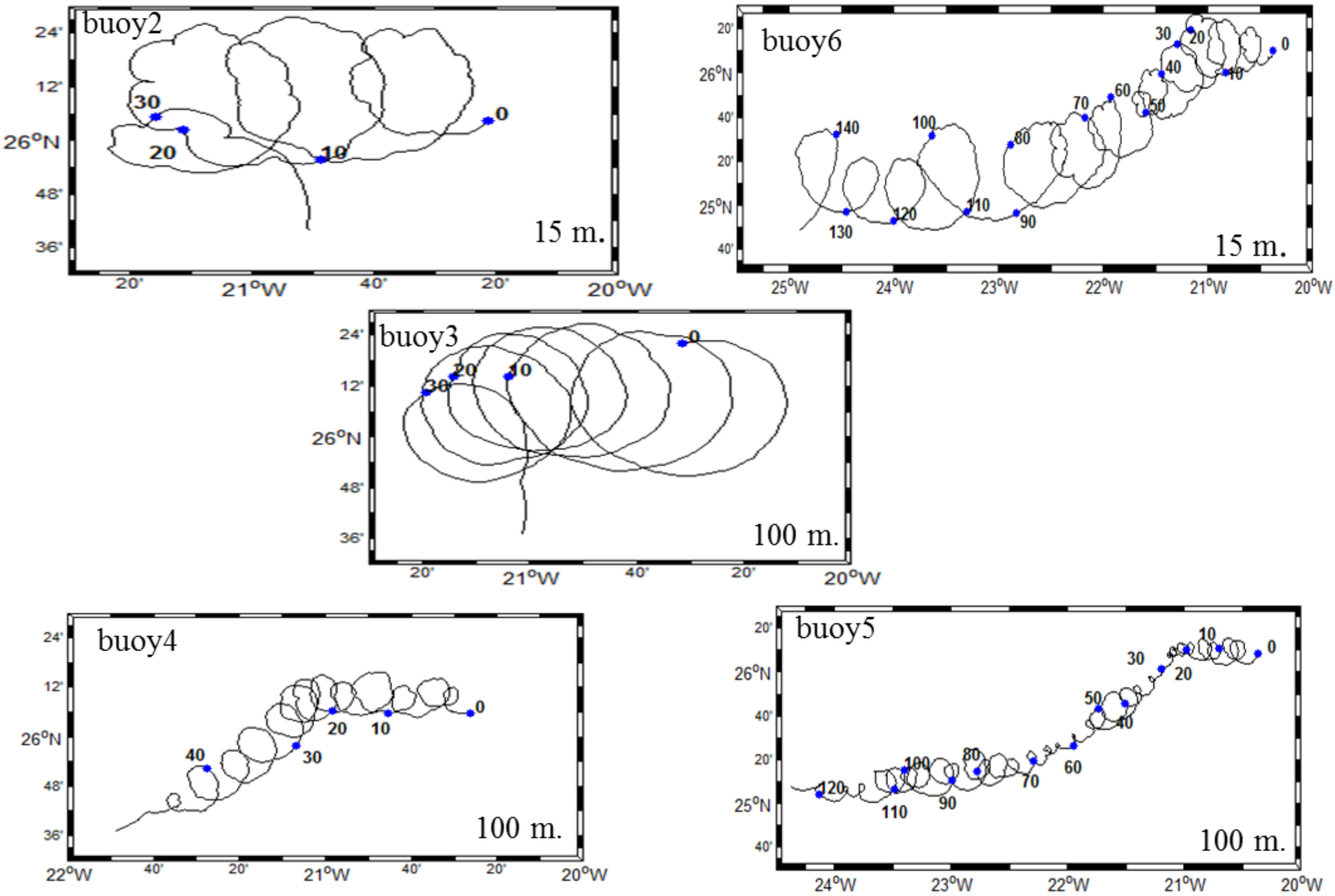

Figure 3. Full buoys trajectories within the eddy. The numbers indicate the days (multiples of 10) elapsed after the buoys deployment. Dots are drawn every 10 days. Drogue depth is also indicated. Day 0 corresponds to 14 of September 2014.

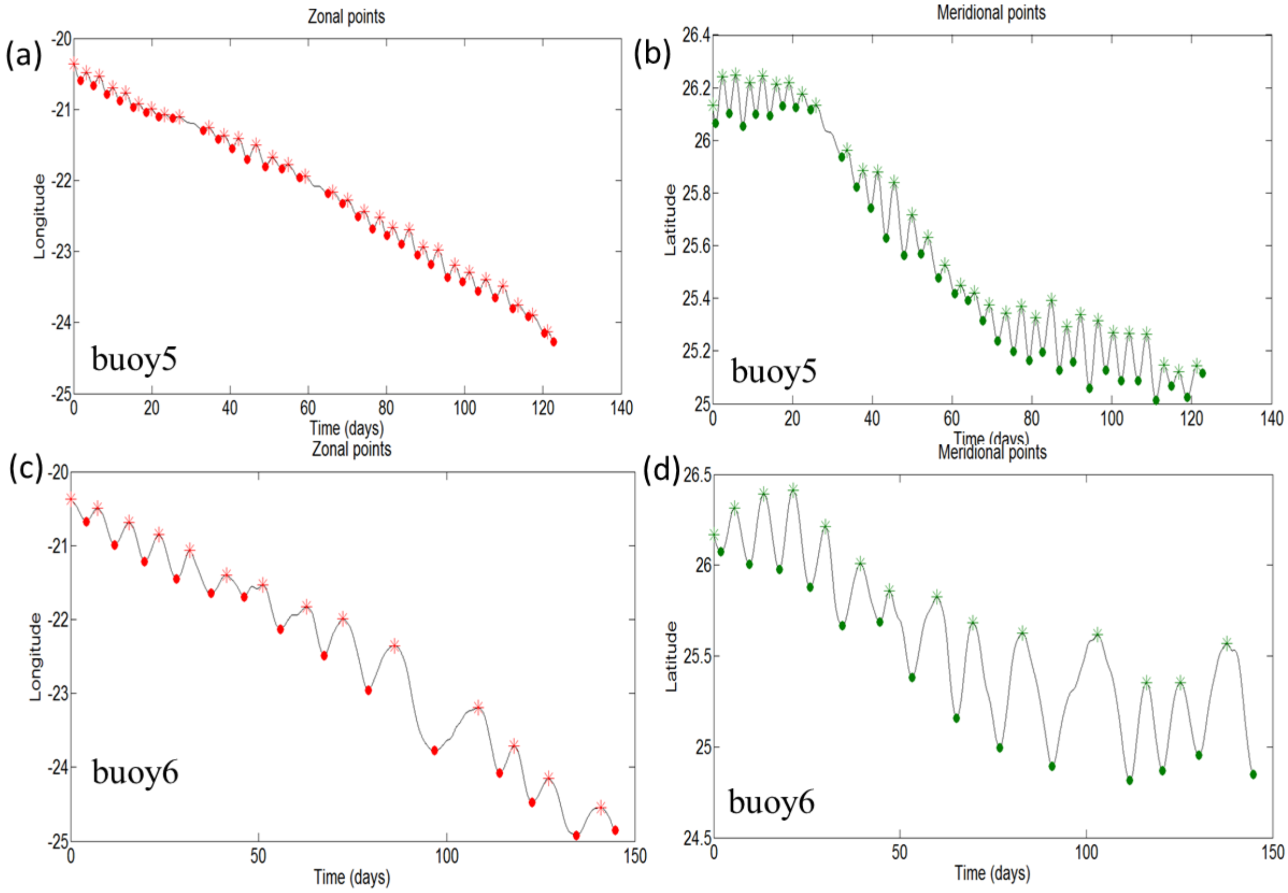

Figure 4. (a),(c) Maxima and minima points of longitude and (b),(d) latitude trajectory for buoys 5 and 6.

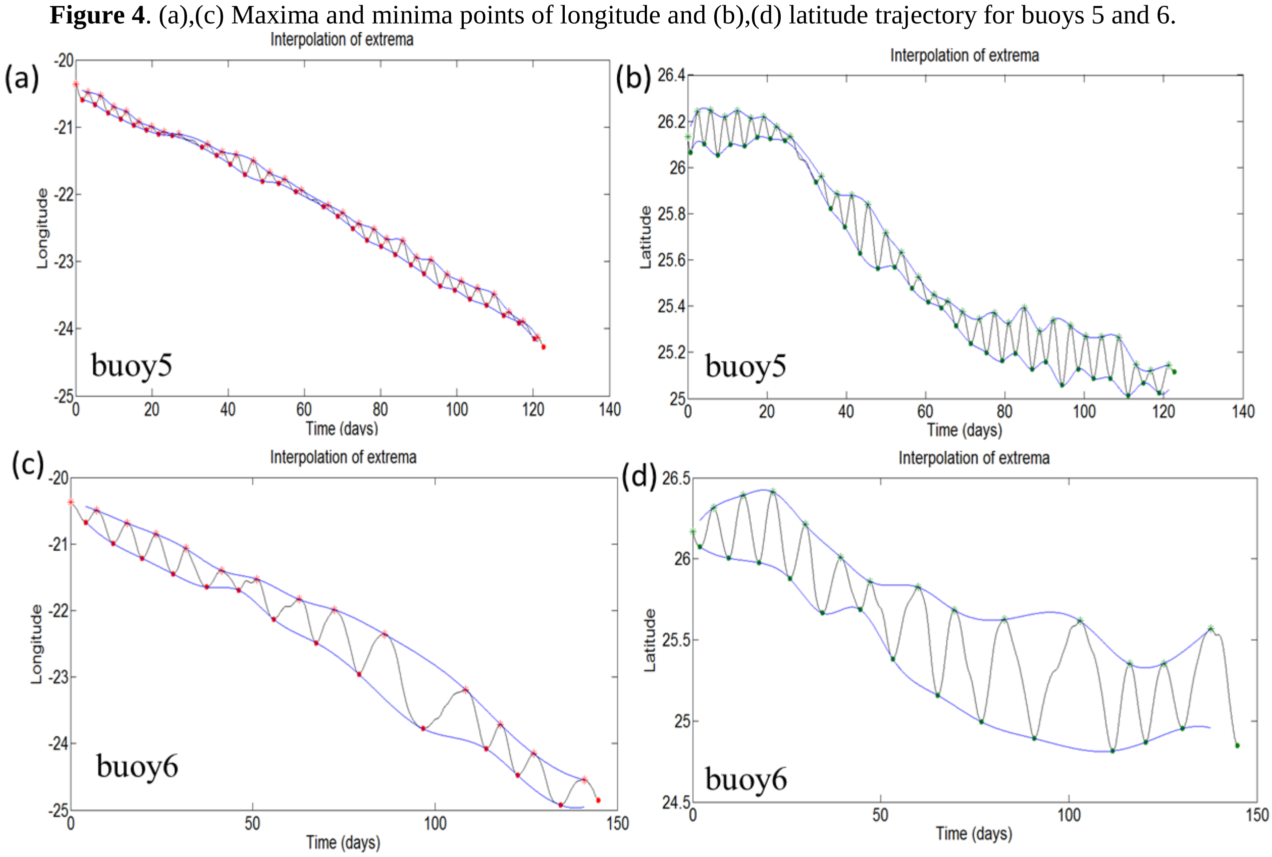

Figure 5. (a),(c) Extrema interpolation of latitude and (b),(d) longitude for buoys 5 and 6.

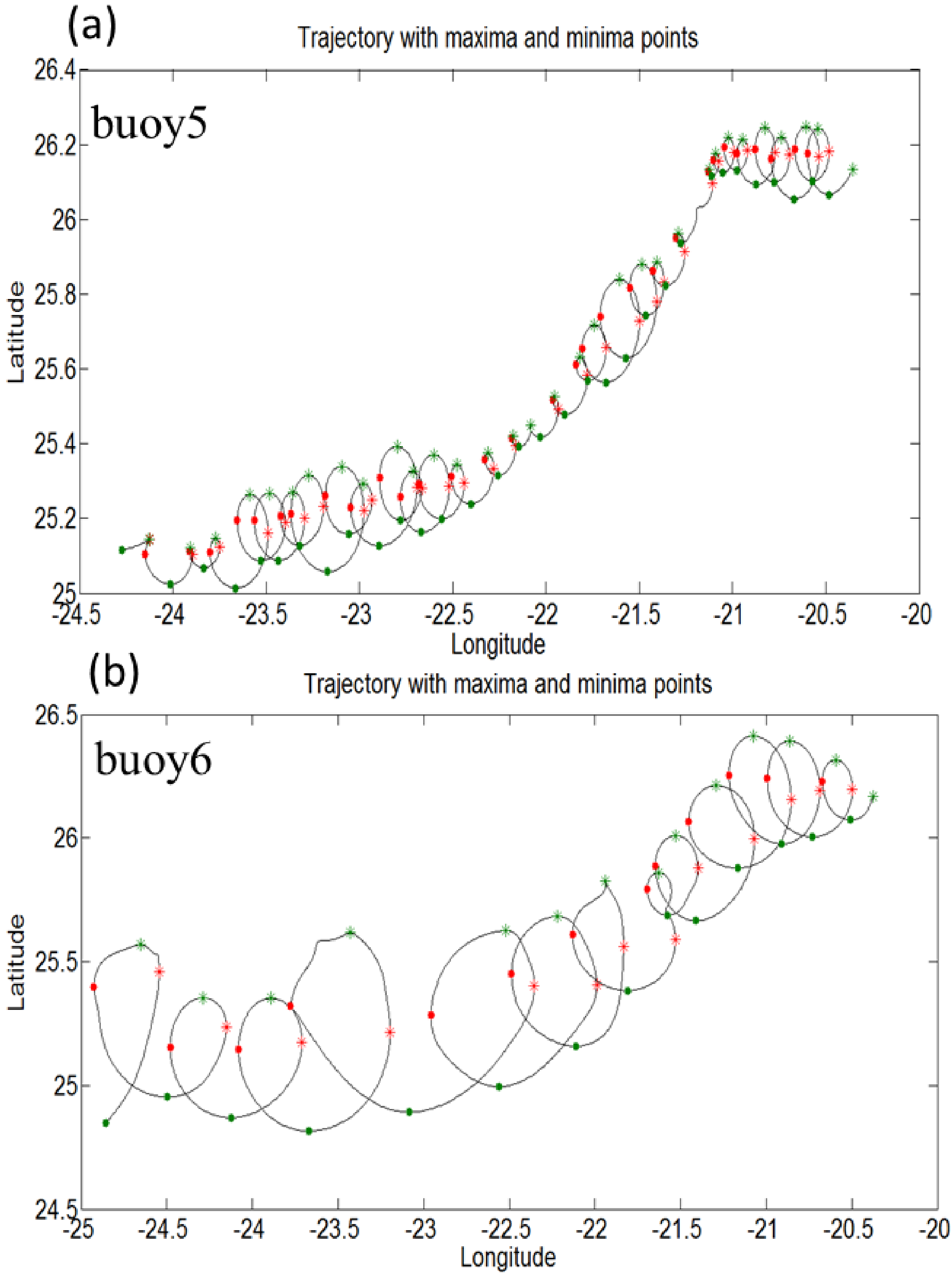

Figure 6. Buoys trajectories with maxima and minima points for longitude and latitude. (a) Buoy5. (b) Buoy6.

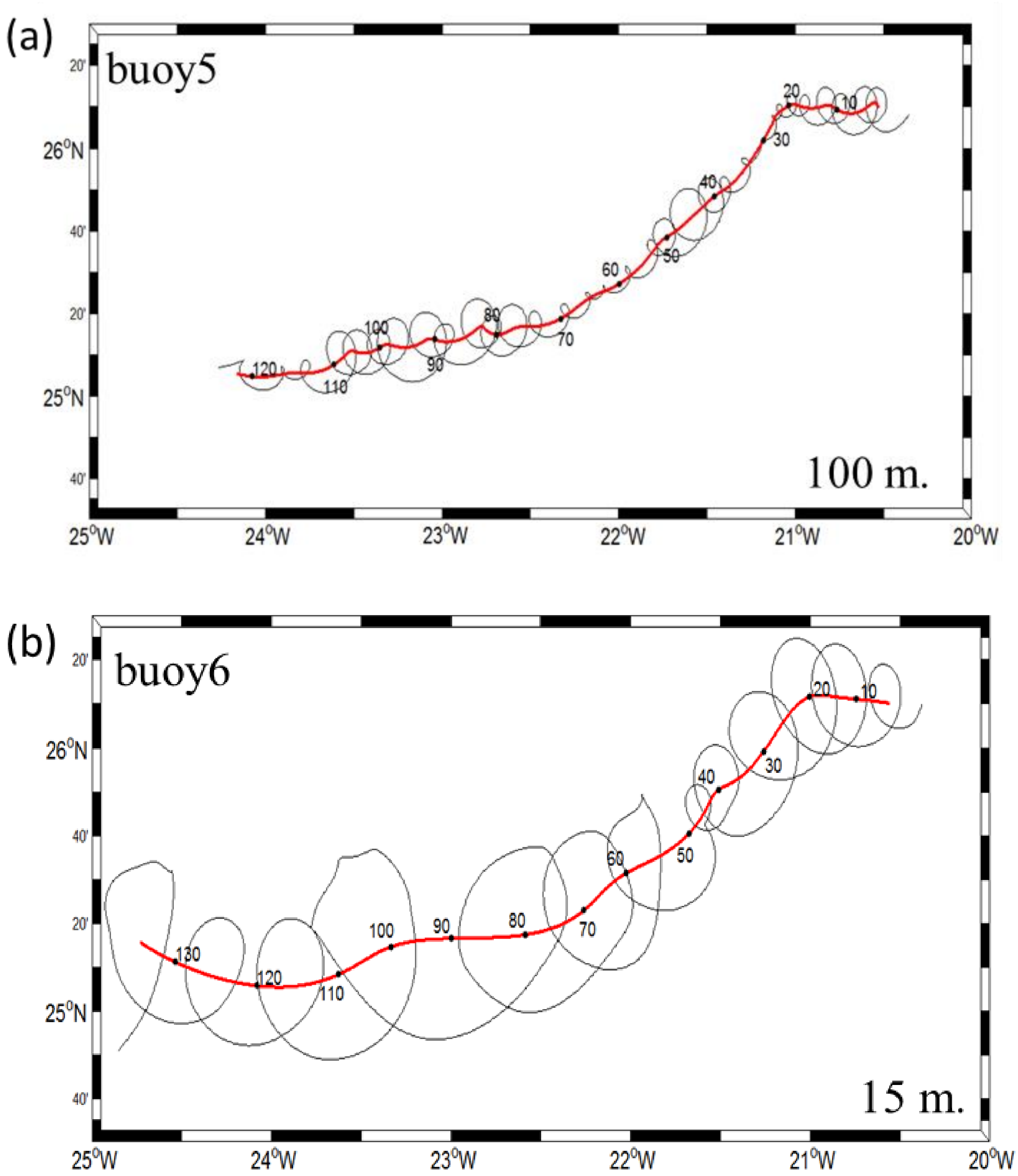

Figure 7. Temporal evolution of the eddy center as traced (red line) by (a) buoy 5 and (b) buoy 6 superposed to full trajectory (black line). The numbers indicate the days (multiples of 10) elapsed after the buoys deployment. Dots are drawn every 10 days.

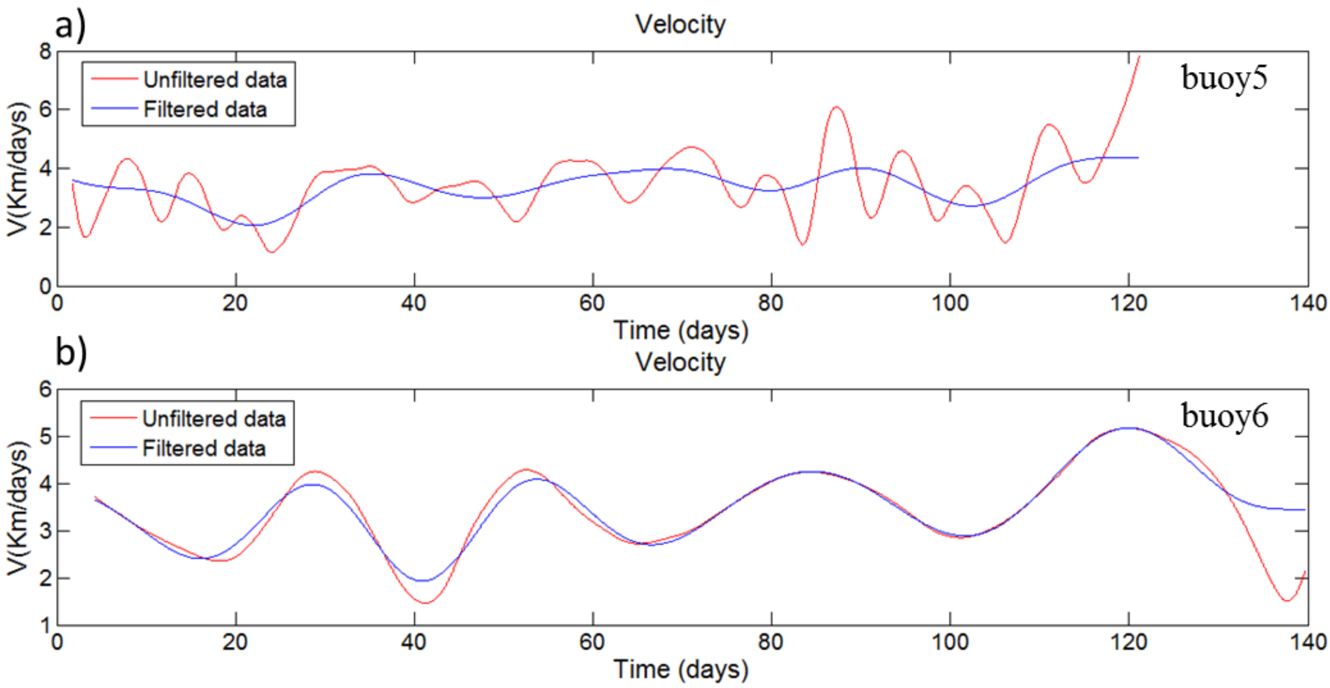

Figure 8. Speeds of the eddy center unfiltered (red line) and 10 days filtered (blue line) for (a) buoy 5 and (b) buoy 6.

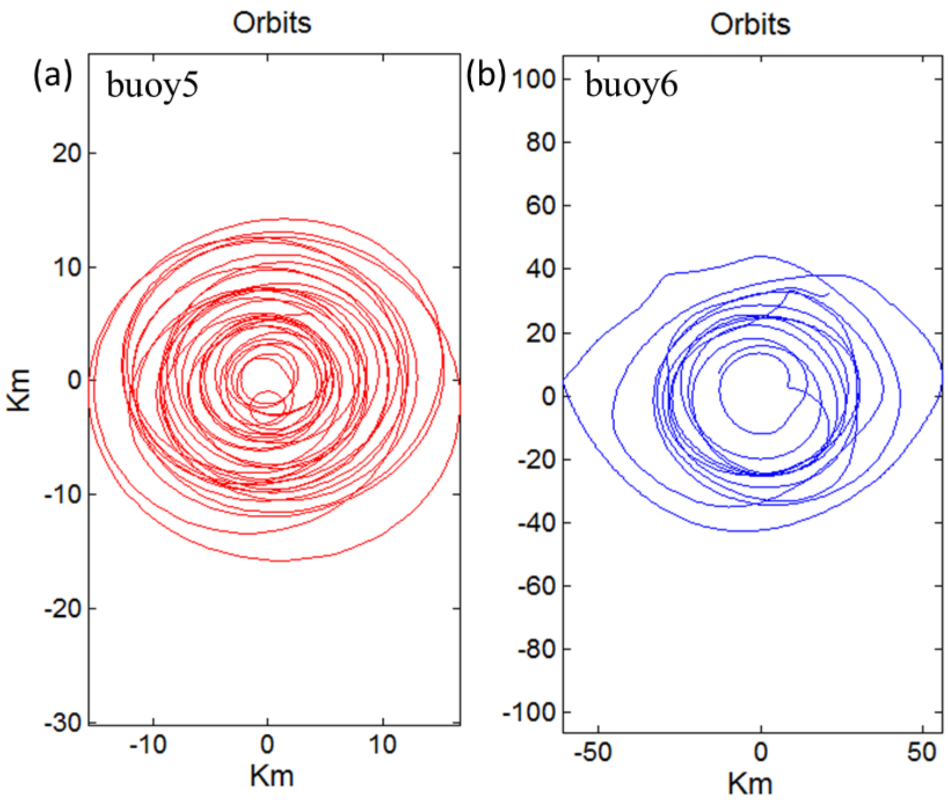

Figure 9. Buoys' orbits corresponding to the complete buoys' time series. (a) Buoy 5. (b) Buoy 6.

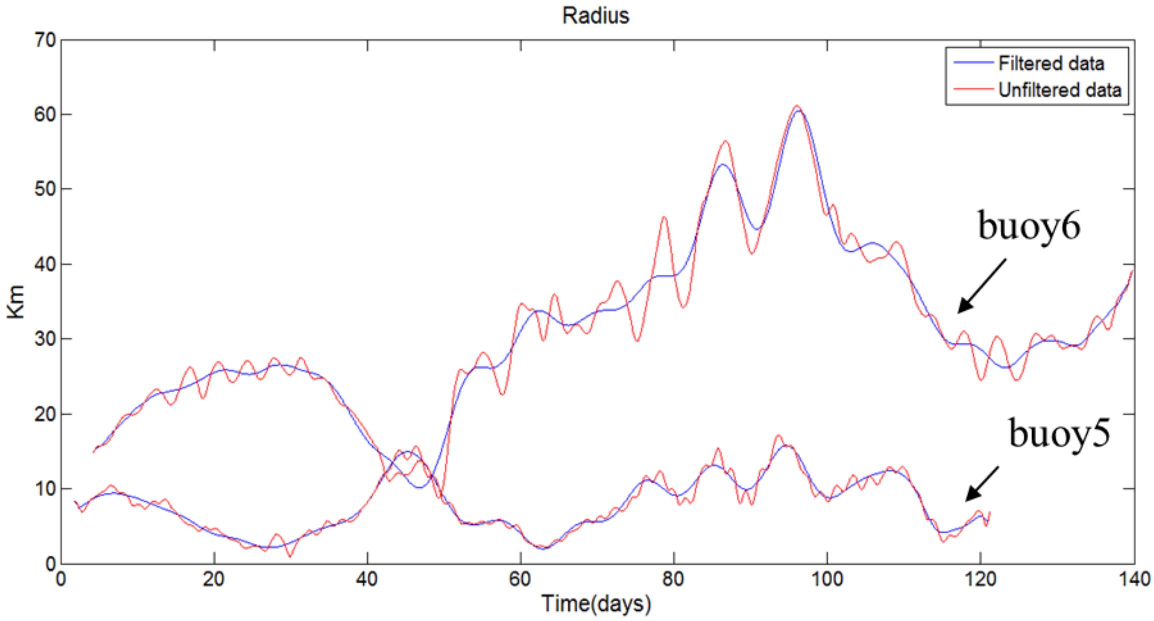

Figure 10. Instantaneous (red line) and mean (blue line) orbital radius for buoy 5 and buoy 6.

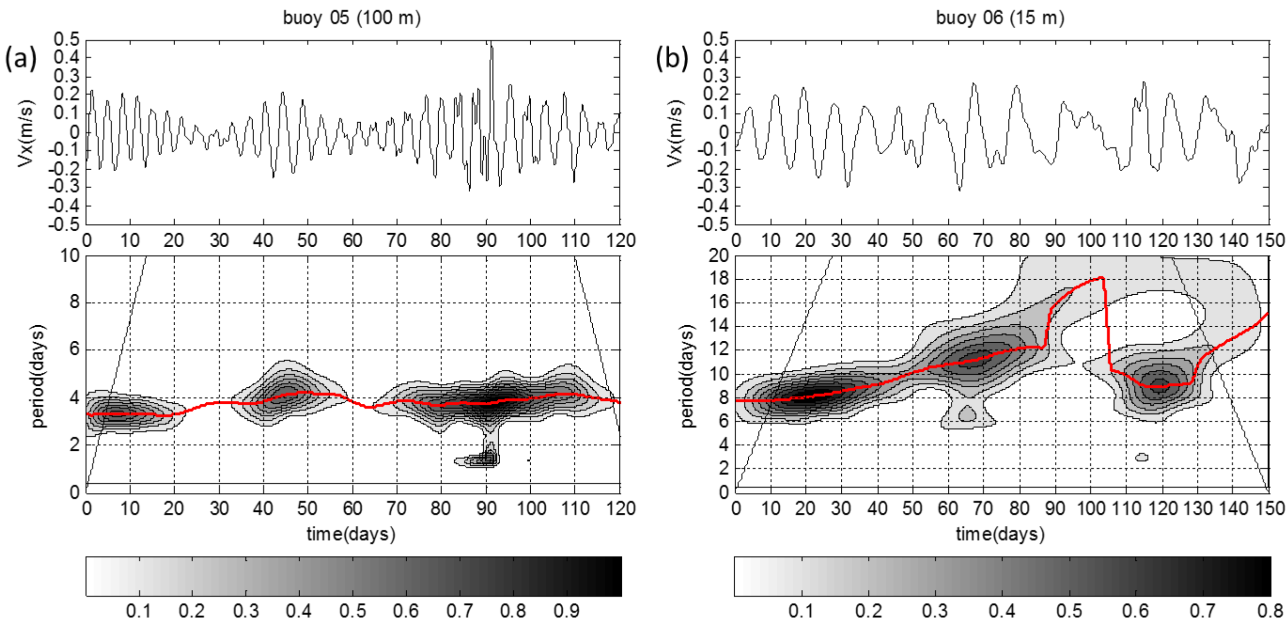

Figure 11. Upper panels, zonal velocities (eastward positives) for buoys (a) 5 and (b) 6. Lowers panels, kinetic energy spectra as a function of time as obtained from the wavelet analysis of the zonal velocities for buoys (a) 5 and (b) 6.

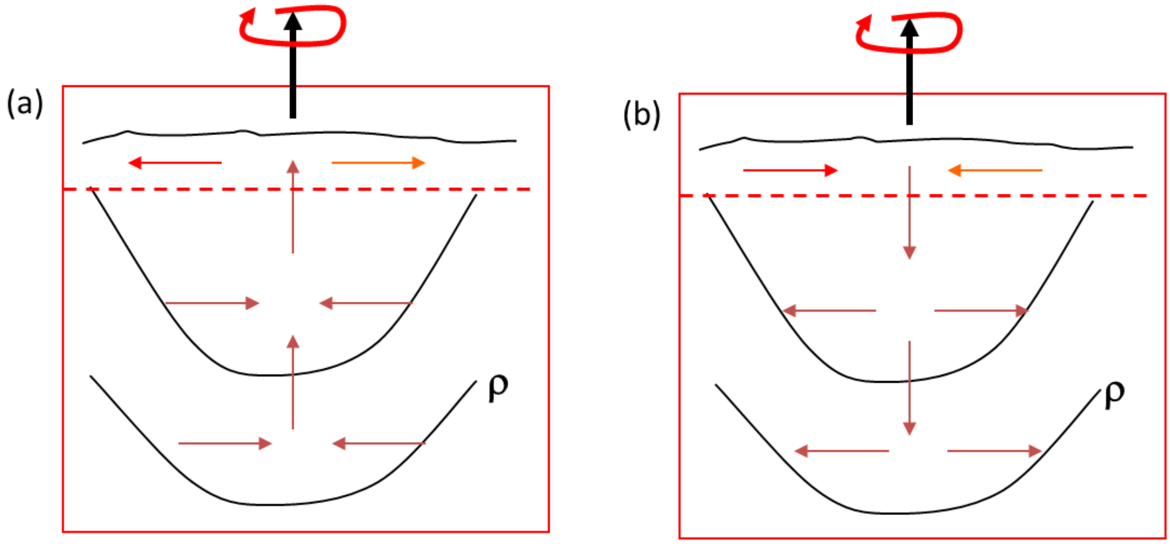

Figure 12.Schemtics of the secondary circulation for (a) upwelling mode and (b) downwelling mode.

6. Actividades realizadas

Las actividades desarrolladas para la realización del Trabajo de Fin de Título (TFT) se llevaron a cabo en el Departamento de Física, bajo la supervisión de mi Tutor, Pablo Sangrà Inciarte y de mi Co-Tutora, Diana Grisolía Santos. Las actividades realizadas fueron las siguientes:

1) Reunión inicial. Planificación y temporalización.

   En esta primera reunión establecimos las características a analizar relacionadas con el remolino PUMP, así como los objetivos a alcanzar en el TFT. También realizamos un cronograma con las horas de reuniones, para verificar la evolución de las tareas, y las horas de trabajo conjuntas e individuales necesarias para completar las distintas actividades. Por último especificamos los conocimientos que tendría que repasar y adquirir para un buen desarrollo del TFT.

2) Revisión bibliográfica.

   Mi Tutor de Empresa me seleccionó una serie de artículos, para tener un primer contacto con el campo de estudio, los cuales luego se irían ampliando a medida que fuera necesario, estos fueron:

- Sangrà, P., Pelegrí, J. L., Hernández-Guerra, A., Arregui, I., Martín, J. M., Marrero-Díaz, A., Martínez, A., Ratsimandresy, A. W., Rodríguez-Santana, A., (2005). Life History of an anticyclonic eddy. *Journal of Geophysical Research*, 11, C03021.
- Sangrà, P., Auladell, M., Marrero-Díaz, A., Pelegrí, J.L., Fraile-Nuez, E., Rodríguez-Santana, A., Martín, J. M., Mason, E. and Hernández-Guerra, A., (2007). On the nature of oceanic eddies shed by the Island of Gran Canaria. *Deep-Sea Research I*, 54, 687-709.
- Sangrà, P., Pascual, A., Rodríguez-Santana, A., Machín, F., Mason, E., McWilliams, J. C., Pelegrí, J. L., Dong, C., Rubio, A., Arístegui, J., Marrero-Díaz, A., Hernández-Guerra, A., Martínez-Marrero, A. and Auladell, M., (2009). The Canary Eddy Corridor: a major pathway for long-lived eddies in the subtropical North Atlantic. *Deep-Sea Research I*, 56, 2100-2114.

3) Programación Matlab.

   Para esta actividad me leí el manual sobre "Modelos en Oceanografía Física. Parte I: Fundamentos de Programación con Matlab", elaborado por Antonio Martínez Marrero, para repasar mis conocimientos y poder realizar los ejercicios propuestos por mi Tutor. Además aprendí a utilizar el *M_Map: A mapping package for Matlab*, una herramienta para la realización de gráficas con un formato determinado y que me fue de gran utilidad en las gráficas realizadas para mi Trabajo de Fin de Grado.

4) Análisis lagrangiano de un remolino.

En esta parte conté con la ayuda de mi Tutor, Pablo Sangrá Inciarte y de mi Co-Tutora, Diana Grisolía Santos. Con ellos aprendí como tratar los datos y el cálculo de distintas variables relacionadas con las boyas, útiles a la hora de estudiar determinadas características de los remolinos, como pueden ser el periodo, la velocidad, la trayectoria, la trayectoria media, las órbitas y las velocidades zonales mediante análisis wavelet. Diana me recomendó la lectura de:

- "Brassington, G. B., (2010). Estimating surface divergence of ocean eddies using observed trajectories from a surface drifting buoy. *Journal of Atmospheric an Oceanic Technology*, 27, 705-720."

En este artículo se detalla la realización de un método para el cálculo de la trayectoria media de la boya, mediante el cálculo de máximos y mínimos. Para ello se debe realizar, entre otros cálculos, la descomposición de las órbitas trazadas por las boyas en un movimiento armónico simple. Esta fue una de las actividades que requirió más tiempo, ya que el método de Brassington presenta una cierta complejidad y obtuvimos una serie de errores que tuvimos que ir solucionando a medida que aparecían.

5) Realización del Trabajo de Fin de Título.

Comencé con los Resultados que se fueron redactando conjuntamente con la Metodología a medida que obtenía las gráficas, las cuales iba comentando con la supervisión de mi Tutor, a medida que se presentaban las definitivas. Una vez finalizados estos dos apartados continúe con los restantes, añadiendo siempre la bibliografía según la leía.

7. Formación recibida

En un primer momento se consideró la posibilidad de trabajar los datos mediante el programa Fortran, por lo que comencé a informarme sobre la utilización de este, previo comienzo del TFT. En la primera reunión acordamos trabajar sólo con el programa Matlab, ya que lo conocía de antemano debido a su utilización en las clases relacionadas con el campo de la Física (Ondas, Oceanografía Física, etc.).

Amplié las enseñanzas recibidas gracias a mi Tutor y a mi Co-Tutora, en la programación en Matlab, así como en el cálculo de datos y en la realización de gráficas, que me ayudó con la aportación de trabajos previos realizados por ellos y con material didáctico. Además pude conocer una herramienta básica a la hora de graficar con Matlab, como es el *M_Map: A mapping package for Matlab*, del cual había desconocido su existencia durante los distintos cursos académicos.

8. Nivel de integración e implicación dentro del departamento

La relación con el Tutor, y con la Co-Tutora, así como con los distintos participantes del proyecto PUMP fue en todo momento respetuosa y cordial. Gracias a mi Tutor tuve contacto con la mayoría de los integrantes del Proyecto PUMP, ya que habían algunos que no se encontraban presentes, aunque sin embargo pudieron asistir a alguna de las reuniones post-campaña, como fue el caso de Enric Pallàs y Des Barton. Además fui invitada a las distintas reuniones post-campaña que se llevaron a cabo para establecer pautas de trabajo y a las cenas organizadas tras las reuniones. En estas reuniones pude apreciar el grado de colaboración, integración y relación entre todos los campos de la Oceanografía Física y de esta con los grupos de Oceanografía Biológica.

Desde el primer momento me sentí muy acogida por todos los componentes, los cuales no dudaban en ayudarme cuando me surgían dudas o tenía dificultades. También conocí a los estudiantes post-doctorales a cargo de mi Tutor, con ellos conseguí ampliar mi visión del grado en Ciencias del Mar y esto me hizo replantearme las ramas de las Oceanografía Física a las que podría dedicarme en un futuro.

Mi nivel de integración dentro del departamento se observa en mi asistencia a las reuniones post-campaña y en la colaboración junto con Diana Grisolía-Santos, Pablo Sangrà, Antonio Martínez-Marrero, Luis Cana, Bárbara Barceló en la realización del póster "Lagrangian evolution of a mid ocean anticyclonic eddy", el cual se presentará en la **26th International Union Geodesy and Geophysics (IUGG) General Assembly 2015** celebrado en Praga, República Checa del 22 de Junio al 2 de Julio del 2015. Este se basa en algunas de las partes estudiadas durante la realización de mi TFT.

9. Aspectos positivos y negativos más significativos relacionados con el desarrollo del TFT

Los aspectos a destacar durante la realización del TFT han sido todos positivos, ya que desde un primer momento recibí una grata integración por parte de todos los integrantes del departamento y no tuve ningún problema en el acceso al material necesario para la realización del mismo, así como en la facilidad a la hora de contactar con los distintos miembros.

10. Valoración personal del aprendizaje conseguido a lo largo del TFT

Mi valoración final a cerca del TFT realizado con mi Tutor y mi Co-Tutora ha sido satisfactoria desde el primer momento. Conté con un gran apoyo por parte de todos los miembros, que no dudaron en ayudarme siempre que lo necesitaba y en aportarme información que pudiera ser de utilidad para el desarrollo del TFT.

Por otro lado mis conocimientos y mi experiencia en el campo de la investigación se han visto incrementados enormemente, al verme incluida, desde un primer momento, en una campaña oceanográfica abarcada bajo el Proyecto PUMP. A pesar de que entré a formar parte una vez finalizada la campaña en mar, en las reuniones pude ampliar mi visión acerca de las distintas actividades y tareas desempeñadas a bordo del buque oceanográfico Hespérides, también disfruté del relato de distintas anécdotas que tuvieron lugar durante la campaña en mar, aportadas por gran parte de los integrantes.

Por último destacar la labor ejercida por mi Tutor, Pablo Sangrà, y mi Co-Tutora, Diana Grisolía, sin los cuales no habría obtenido un resultado tan satisfactorio durante la elaboración del TFT.